ISSN 0006-2979, Biochemistry (Moscow), 2009, Vol. 74, No. 4, pp. 406-415. © Pleiades Publishing, Ltd., 2009.
Original Russian Text © E. V. Sidorin, R. H. Ziganshin, G. A. Naberezhnykh, G. N. Likhatskaya, E. V. Trifonov, S. D. Anastiuk, O. V. Chernikov, T. F. Solov'eva, 2009, published in Biokhimiya, 2009, Vol. 74, No. 4, pp. 501-514.
Originally published in Biochemistry (Moscow) On-Line Papers in Press, as Manuscript BM08-262, February 8, 2009.

Chaperone Skp from *Yersinia pseudotuberculosis* Exhibits Immunoglobulin G Binding Ability

E. V. Sidorin[1]*, R. H. Ziganshin[2], G. A. Naberezhnykh[1], G. N. Likhatskaya[1], E. V. Trifonov[3], S. D. Anastiuk[1], O. V. Chernikov[1], and T. F. Solov'eva[1]

[1]*Pacific Institute of Bioorganic Chemistry, Far East Division of the Russian Academy of Sciences, pr. 100-letiya Vladivostoka 159, 690022 Vladivostok, Russia; fax: (4232) 314-050; E-mail: sev1972@mail.ru*
[2]*Shemyakin–Ovchinnikov Institute of Bioorganic Chemistry, Russian Academy of Sciences, ul. Miklukho-Maklaya 16/10, 117991 Moscow, Russia; fax: (495) 335-7103*
[3]*Institute for Automation and Control Processes, Far East Division of the Russian Academy of Sciences, ul. Radio 5, 690041 Vladivostok, Russia*

Received August 12, 2008
Revision received November 27, 2008

Abstract—A low-molecular-weight cationic protein that can bind human and rabbit immunoglobulins G has been isolated from *Yersinia pseudotuberculosis* cells. This immunoglobulin binding protein (IBP) interacts with IgG Fc-fragment, the association constant of the resulting complex being 3.1 μM^{-1}. MALDI-TOF mass spectrometry analysis of IBP revealed its molecular mass of 16.1 kDa, and capillary isoelectrofocusing analysis showed p*I* value of 9.2. N-Terminal sequence determination by Edman degradation revealed the sequence of the 15 terminal amino acid residues (ADKIAIVNVSSIFQ). Tryptic hydrolysate of IBP was subjected to MALDI-TOF mass spectrometry for proteolytic peptide profiling. Based on the peptide fingerprint, molecular mass, p*I*, and N-terminal sequence and using bioinformatic resources, IBP was identified as *Y. pseudotuberculosis* periplasmic chaperone Skp. Using the method of comparative modeling a spatial model of Skp has been built. This model was then used for modeling of Skp complexes with human IgG1 Fc-fragment by means of molecular docking.

DOI: 10.1134/S0006297909040087

Key words: chaperone Skp, immunoglobulin-binding protein, immunoglobulin G, Fc fragment of IgG, computer modeling

Molecular chaperones are highly conserved proteins that promote correct formation of spatial structure of other proteins. Binding with chaperones prevents premature association of newly formed proteins with each other and also with other proteins and favors native folding.

Good evidence now exists that Skp (seventeen kilodalton proteins) are bacterial periplasmic chaperones that are involved in biogenesis of outer membrane proteins of Gram-negative bacteria [1-8]. They are widely distributed among enterobacteria and form a family of homologous low-molecular-weight proteins (14-20 kDa) with marked basic properties (p*I* 9-10) [9-14]. Based on analysis of genomic sequences, the presence of Skp was predicted in pathogenic bacteria belonging to the genus *Yersinia* including *Y. pseudotuberculosis*. The *Y. pseudotuberculosis skp* gene was cloned, sequenced, and the amino acid sequence of the protein product was deduced [15, 16].

Besides interacting with outer membrane proteins as a chaperone, Skp exhibits other properties that might be of biological and physiological importance. Skp proteins demonstrate lipopolysaccharide- and DNA-binding activity [9-12], and they act as chemoattractants for monocytes and polymorphonuclear leukocytes [17]. It is also suggested that these proteins exhibit antigenic properties underlying serologic cross-reactivity with human histocompatibility antigen HLA-B27 [16].

Immunoglobulin binding proteins (IBP) are considered as important factors of bacterial pathogenicity. It is believed that interaction between IBP and immunoglobulins decreases opsonization and phagocytosis of bacteria and prevents complement binding; these factors can help bacteria to escape interaction with the host immune system. IBP is a heterogeneous family of proteins differing

Abbreviations: IBP, immunoglobulin binding protein; Skp, seventeen kilodalton protein.

* To whom correspondence should be addressed.

by localization in bacteria, molecular structure, and immunoglobulin binding activity [18, 19].

We demonstrated earlier that *Y. pseudotuberculosis* cells are characterized by the presence of proteins that can bind immunoglobulins G (IgG). During blot analysis, IBP appear as several bands with molecular masses from 7 to 20 kDa [20, 21]. One of these proteins, the immunoglobulin binding protein of 14.3 kDa, has been isolated and characterized [20].

In this work, we describe isolation and characterization of a new IBP protein of 16 kDa; this IBP-16 protein from *Y. pseudotuberculosis* has been identified as chaperone Skp. We have investigated binding of Skp with rabbit and human IgG and built a model of the spatial structure of *Y. pseudotuberculosis* Skp and its complex with human IgG1 Fc-fragment.

MATERIALS AND METHODS

The following materials and chemicals were used in this study: columns Source 15S (Pharmacia Biotech, Sweden), HiTrap Desalting (Amersham Biosciences, Sweden), and Zorbax Eclipse XDB-C8 (Agilent, USA); acrylamide (Serva, Germany), trypsin (Promega, USA), ultrafiltration membranes Ripore (Olaine, Latvia), acetonitrile (grade 2; Cryochrome, Russia), nitrocellulose membrane (Sartorius, Germany), polyethylene glycol 3000 Da (Merck, Germany), ampholytes (pH 7-9) (LKB, Sweden) and (pH 9-11) (Serva), human IgG and Fc-fragment of human IgG (ICN Biomedicals, USA), rabbit IgG conjugated with horseradish peroxidase (ICN Biomedicals), *S. aureus* protein A (Sigma, USA), plates for enzyme-linked immunosorbent assay (MaxiSorp; Nunc, Denmark). All other chemicals of chemically pure grade produced by Reakhim (Russia) were used without additional purification.

Buffers A (50 mM Tris-HCl, pH 8.0) and B (50 mM CH_3COONa/CH_3COOH, pH 5.0) were used as buffer systems.

Microorganisms and conditions of bacterial cultivation. The *Y. pseudotuberculosis* strain 598 serovar 1B was used. Conditions of the bacterial cultivation are described by Ovodov et al. [22].

SDS-PAGE. Polyacrylamide gel electrophoresis in the presence of SDS was performed by the method of Laemmli [23]. All samples for electrophoresis were prepared without heating at 100°C. Proteins with molecular masses of 11, 17, 24, 33, 40, 55, 72, 100, and 130 kDa (Fermentas, Lithuania) were used as molecular mass markers. The proteins separated in the gel were stained with a Coomassie R-250 solution in 10% acetic acid and 45% ethanol.

Methods of chemical analysis. Total protein content was determined by the Bradford method [24] using lysozyme as a standard.

Isolation of IBP from the pseudotuberculosis microbe. Before cell disruption, acetone powder of the microbial mass of *Y. pseudotuberculosis* was treated with phosphate buffered saline (PBS), pH 7.2, under vigorous mixing with glass beads for 30 min at room temperature followed by subsequent centrifugation at 3000*g* for 20 min at 20°C. This procedure removes capsule material of these cells [25]. Bacterial cells were disrupted by means of combination of two methods: freeze–thawing and ultrasound disintegration. For the freeze–thawing procedure cell suspension (15.4 g) in 100 ml of buffer A was frozen and kept overnight at –20°C. The next day the sample was thawed at room temperature and sonicated using a UZDN-2T ultrasound disintegrator (44 kHz, 30 min and 4-10°C) followed by subsequent centrifugation at 10,000*g* for 10 min at 20°C. For better disruption of bacterial cells, the combination of these methods was repeated twice. IBP was extracted by sequential treatment of disrupted bacteria with buffer A and buffer B for 30 min at 20°C followed by subsequent centrifugation for 10,000*g* for 20 min at 20°C after each extraction. Protein extraction was monitored by changes in absorbance at 280 nm.

Ion-exchange chromatography. The extract in buffer B (400 ml) filtered through a filter (pore size of 0.22 μm) was applied onto a Source 15S column for ion-exchange chromatography. The chromatography was carried out using the column equilibrated with buffer B and an FPLC chromatograph (Amersham Pharmacia Biotech). After column loading, it was then washed with 10 ml of buffer B to remove weakly bound proteins. The ion-exchange chromatography procedure employed two modes of protein elution: isocratic elution and a continuous gradient of NaCl in buffer B. Isocratic elution was carried out at 0.2, 0.4, 0.6, and 2 M NaCl in buffer B (2.5, 1.5, 1.5, and 4.5 ml, respectively), and the gradient elution was carried with a continuous gradient of NaCl from 0.6 to 2 M (2 ml). Fractions of 0.5 ml were collected at the elution rate of 0.5 ml/min. The fractions were analyzed for immunoglobulin binding activity by means of the dot method. The active fractions were pooled (by results of SDS-PAGE) and concentrated by ultrafiltration on membranes with the exclusion limit of 1000 Da (Ripore, Latvia). After concentrating, gel filtration was additionally performed on a HiTrap Desalting column in buffer B.

High performance reverse-phase chromatography. Fractions obtained after cation-exchange chromatography and containing active protein were used as samples for subsequent purification. Before application onto a column, these samples were filtered through a filter with 0.22 μm pores. The chromatographic procedure was carried out using an Agilent HPLC-chromatograph and a Zorbax Eclipse XDB-C8 column equilibrated with 15% acetonitrile in 0.1% TFA (v/v). The bound protein was eluted from the column by gradients of acetonitrile 15-35, 35-43, 43-100, and 100% (2, 8, 1, and 2 ml, respectively). Usually the rate of elution was 1 ml/min, and only in the

case of acetonitrile gradient 35-43% the elution rate was reduced to 0.5 ml for better separation of closely eluting peaks. The volume of collected fractions was 0.2 ml.

MALDI-TOF mass spectrometry. Mass spectrometry was performed using a Biflex III MALDI-TOF spectrometer (Bruker, USA) in the positive ion linear mode. Sinapinic acid (3,5-dimethoxy-4-hydroxy-cinnamic acid) matrix was prepared at 10 mg/ml in acetonitrile containing 0.1% trifluroacetic acid. Protein samples after reverse-phase chromatography were applied onto a matrix-covered target by the dried droplet method.

Capillary isoelectrofocusing. This experiment was carried out using the method of isoelectrofocusing (IEF) in an uncoated capillary [26] with some modifications. The major difference consisted in application of a mixture of sample components and carrier ampholytes to the capillary: under our experimental conditions a protein sample, protein markers, and ampholytes were applied to the capillary as one mixture, rather than separate sequential zones. The experiment was carried out using an Agilent capillary electrophoresis system equipped with a diode-array detector and uncoated capillary (d = 50 μm, L_{ef} = 40.5 cm, L_{total} = 48.7 cm) at 20°C. Suppression of electroosmotic flow and reduction of protein band diffusion were achieved by addition of polyethylene glycol (PEG) 3000 Da. Solutions of 0.1 M NaOH and 0.08 M H_3PO_4 containing 0.4% PEG were used as catholyte and anolyte, respectively. Isoelectric point (p*I*) was determined using a protein sample obtained after two sequential cation-exchange chromatography stages and gel filtration as described. The sample applied to the capillary contained 0.4 mg/ml of the analyzed protein, 0.1 mg/ml horse heart myoglobin (p*I* 6.8 and 7.2), 0.1 mg/ml egg lysozyme (p*I* 9.37), 2% ampholytes (pH 7-11), and 0.4% PEG. Before sample application (and between experiments), the capillary was washed with catholyte solution at 995 mbar for 3.5 min (about seven capillary volumes). Sample was injected using hydrodynamic mode under pressure of 50 mbar for 4 min. Isoelectrofocusing and detection were performed at voltage 24 kV for 7 min. After pH gradient formation and protein focusing, proteins were passed from the capillary through the detector by application of 50-mbar pressure. Appearance of protein fractions was monitored by absorbance at 280 and 415 nm.

Analysis of N-terminal amino acid sequence. N-Terminal amino acid sequence of 15 residues was determined in duplicate by automatic Edman degradation on a Procise 492c LC sequencer (Applied Biosystems, USA) equipped with a Series 200 UV/VIS detector (Perkin Elmer, USA) for analysis of phenylthiohydantoyl amino acid derivatives according to the supplier's instructions. Using molecular mass, p*I*, and N-terminal amino acid sequence data, proteins were identified by the TagIdent program and UniProtKB/Swiss-Prot database.

Identification of Skp chaperone using peptide fingerprinting by MALDI-TOF mass spectrometry. A protein sample obtained after reverse-phase hydrophobic chromatography was dissolved (to final concentration of 1 mg/ml) in 50 mM ammonium bicarbonate buffer containing 10% acetonitrile (v/v), and then a trypsin solution (20 ng/μl) was added at ratio 1 : 50 versus the analyzed protein (w/w). The mixture was incubated at 37°C for 12 h, and after addition of 10% (v/v) of 1% TFA, 5 μl of the resulting solution was desalinated on a microcolumn containing a sorbent prepared according to Kilar et al. [27]. One microliter of the eluate of the desalinated sample was mixed with 1 μl of a matrix solution (2,5-dihydroxybenzoic acid, 10 mg/ml, 50% acetonitrile, 0.1% TFA) on a mass spectrometry target. Mass spectra were acquired using an Ultraflex TOF/TOF mass spectrometer (Bruker) in reflection mode in the range of molecular masses from 0.5 to 6 kDa. Protein was identified by peptide fingerprinting using the Mascot software and the Swiss-Prot database of protein sequences. Protein was considered as reliably identified with Mascot protein identification score exceeding 60-70 (http://www.matrixscience.com/help/scoring_help.html).

Methods of determination of immunoglobulin binding activity. Enzyme linked immunosorbent assay (ELISA), dot analysis, and Western blotting were performed using standard methods [28, 29]. Immunoglobulin binding activity of Skp and protein A was determined using a commercially available normal rabbit IgG conjugated with horseradish peroxidase. Optimal protein concentrations for immobilization on plates were determined using a standard dilution method [30]. Molar protein concentrations were calculated assuming molecular masses of Skp and protein A of 16.1 and 42 kDa, respectively. Optimal concentrations of Skp and protein A were 3.5 μM and 4.3 nM, respectively. The results of ELISA analysis were quantified at 492 nm using a μQuant spectrophotometer (Bio-Tek Instruments, USA) and 0.04% solution of *o*-phenylenediamine as a chromogen.

Interaction between Skp and human IgG was inhibited by addition of various concentrations of human IgG Fc-fragments (0.021-0.67 μM); these were added to the well containing immobilized Skp simultaneously with the conjugate human IgG–horseradish peroxidase (0.029 μM). The mixture was incubated at 37°C for 2 h, and binding was determined as described above for determination of the immunoglobulin binding activity of Skp chaperone. The conjugate of human IgG with peroxidase was obtained by the standard periodate method [31]. Binding constant (K_a) was calculated using the formula [32]:

$$A_o/A_i = 1 + K_a \cdot L,$$

where A_o and A_i are light absorbance at zero and L concentration of an inhibitor, respectively.

Computer modeling. The amino acid sequence of *Y. pseudotuberculosis* Skp (serotype O:1b/strain IP31758;

accession number A7FFH8) was obtained from UniProt (http://www.pir.uniprot.org/). Analysis of the amino acid sequence of *Y. pseudotuberculosis* Skp was carried out using tools of the UniProt database. A theoretical model of spatial structure of monomer of *Y. pseudotuberculosis* Skp was generated using the SPDBV program (http://www.expasy.org/spdbv/) [33] and Swiss-Model server (http://swissmodel.expasy.org) [34-36]. Crystal structure of *E. coli* Skp [37], PDB code 1U2M_C [38], was used as a prototype. Energy minimization in vacuum was performed using the GROMACS software version 3.3.1 [39] using GROMOS96 43B1 force field potential.

Molecular docking of Skp was performed with heavy chains of human IgG1 forming Fab and Fc fragments. The structure of the complex of *Y. pseudotuberculosis* Skp monomer with human IgG1 heavy chains was obtained by the method of molecular docking using the GRAMM 1.03 program [40] and a grid unit of 5 Å. Calculations employed the MVS17 cluster (2 × Intel Pentium III, 1 GHz) at the Center of Collective Use the Far Eastern Computational Resource, Far Eastern Branch of the Russian Academy of Sciences. The structure of A and B heavy chains of human IgG1 (residues 1-452 for each chain) was obtained using molecule coordinates (PDB codes 1FC2, 2IG2, 1OQO), and it is similar to the published structure [41]. The complex with the lowest energy among 100 complexes calculated by the GRAMM program was used for structure analysis. The structure of the complex was minimized by the method of Steepest Descent to *E* gradient of 0.01 kJ/mol with OLPS-AA force field by means of the MOE program, version 2007.09 (Chemical Computing Croup, Inc.; http://www.chemcomp.com/). Visualization of molecules and analysis of contacts in the complex were performed using the MOE program.

RESULTS AND DISCUSSION

Isolation and purification of immunoglobulin binding protein. We demonstrated earlier [20, 21], that in the cell envelope of *Y. pseudotuberculosis* there are several proteins of 7-20 kDa, that can bind immunoglobulins in a non-immune manner. One of these IBP with molecular mass of 14 kDa (IBP-14) was isolated and characterized earlier [20]. For isolation of another bacterial IBP, we modified the previously developed scheme of IBP isolation; these modifications mainly involved pretreatment of microbial mass before extraction. For removal of capsule material, cells were stirred in PBS (pH 7.2) with glass beads and then disintegrated using the "freeze–thaw" method and sonication. According to SDS-PAGE and blotting analysis (Fig. 1, a and b, lane *1*), the disintegrated material contained all IBP that were detected earlier in this microbe [20]. It should be noted that subsequent extraction of IBP was performed under rather mild conditions excluding protein denaturation. Cells were sequentially treated with Tris-HCl buffer A (pH 8.0) and acetate buffer B (pH 5.0). The former buffer extracted most proteins lacking immunoglobulin binding activity (data not shown), whereas acetate buffer preferentially extracted a protein detected in the blotting analysis (Fig.

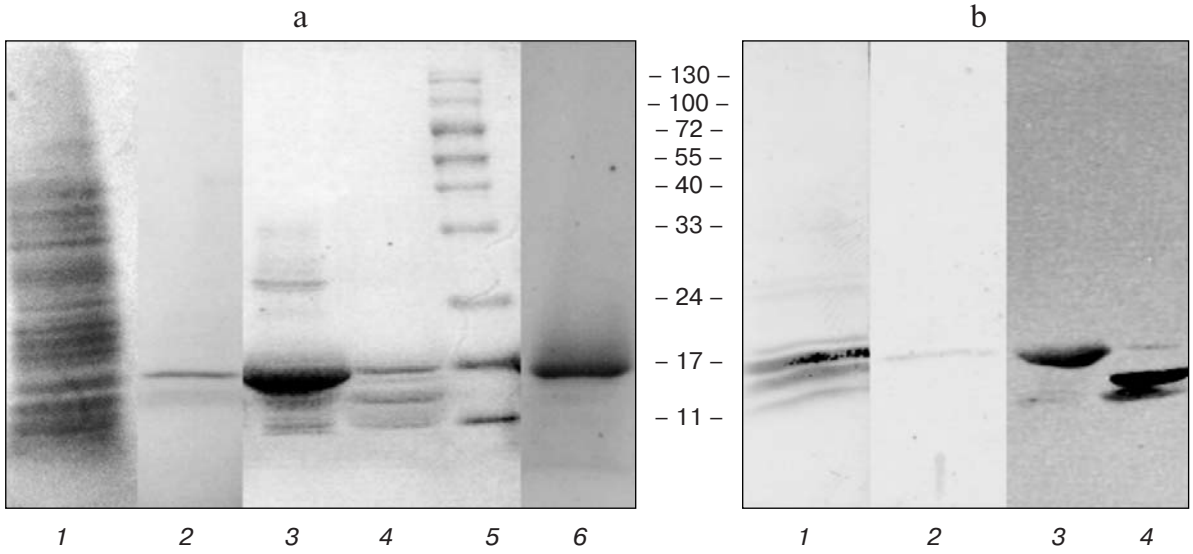

Fig. 1. Electrophoregram of *Y. pseudotuberculosis* proteins in 10-25% gradient SDS-polyacrylamide gel (a) and Western-blot analysis of the same samples detected with rabbit IgG conjugated with horseradish peroxidase (b). Lanes: *1*) disintegrated cells dissolved in 2% SDS; *2*) extract of disintegrated cells in 50 mM sodium acetate buffer, pH 5.0; *3*) IBP eluted from the cation-exchange column by means of NaCl concentrations from 0.3 to 0.4 M in acetate buffer (fraction 1); *4*) IBP eluted from the cation-exchange column by means of NaCl concentrations from 0.4 to 0.7 M in acetate buffer (fraction 2); *5*) protein markers with molecular masses of 11, 17, 24, 33, 40, 55, 72, 100, and 130 kDa; *6*) IBP-16 after rechromatography on the cation-exchange column.

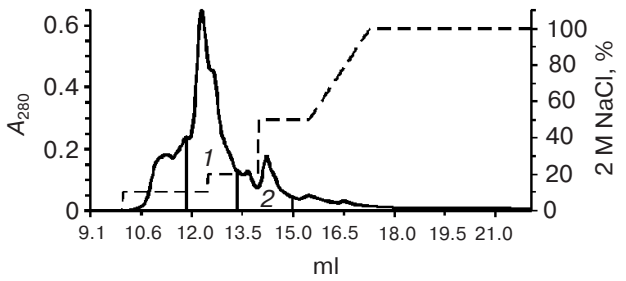

Fig. 2. IBP elution profile from a Source 15S cation-exchange column in 50 mM sodium acetate buffer (pH 5.0). *1*) First total fraction containing active IBP protein; *2*) second total fraction containing active IBP. Protein (A_{280}, solid line); gradient of NaCl concentrations in 50 mM sodium acetate buffer (pH 5.0) (broken line).

1, a and b, lane *2*) as a band in the molecular mass region of 16-17 kDa (IBP-16).

For isolation of this protein, the extract was fractionated by cation-exchange chromatography. The chromatographic procedure was accompanied by concentration of active proteins and their separation into two fractions (Fig. 2, peaks *1* and *2*). The first fraction, which was preferentially eluted during the increase in sodium chloride concentration from 0.3 to 0.4 M, contained mainly IBP-16 (Fig. 1, a and b, lane *3*). The second fraction collected during the increase in ionic strength to 0.7 M NaCl contained IBP with molecular masses of 10 and 14 kDa and some amount of IBP-16 (Fig. 1, a and b, lane *4*). Subsequent purification of IBP-16 was performed by rechromatography of fraction 1 on the cation-exchange column followed by reverse-phase hydrophobic chromatography. IBP-16 protein was eluted at 40% acetonitrile as a single peak.

SDS-PAGE, MALDI-TOF spectrometry, and N-terminal analysis revealed that the resulting preparation was homogeneous IBP-16.

Characteristics and identification of IBP-16. MALDI-TOF analysis of IBP-16 revealed its molecular mass of 16.1 ± 0.006 kDa (Fig. 3). Besides the molecular

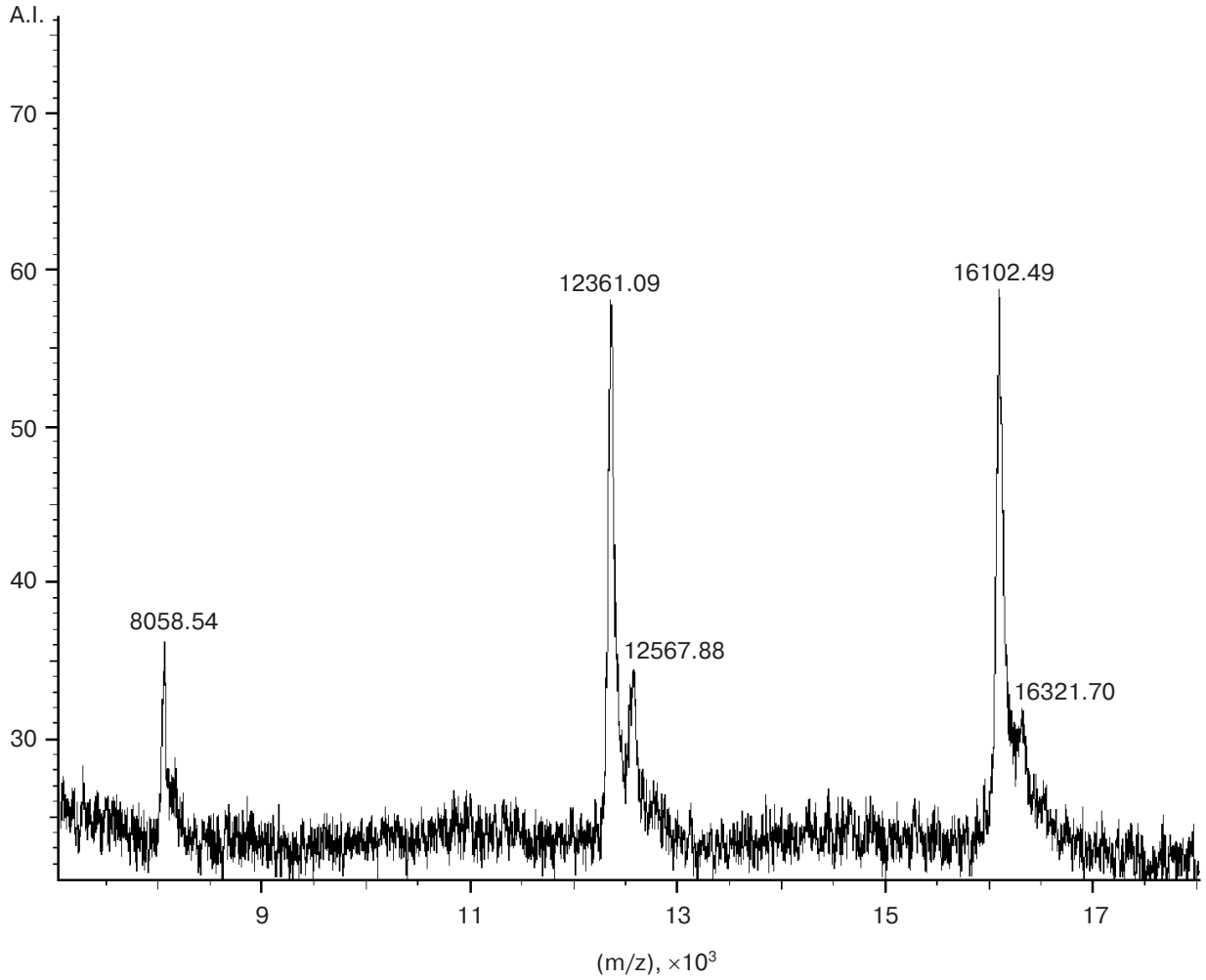

Fig. 3. MALDI-TOF mass spectrum of IBP-16 in 40% acetonitrile in 0.1% TFA. Cytochrome *c* with molecular mass of 12361.09 Da was used for internal calibration.

Table 1. Peptide fingerprint of IBP-16. The result of Mascot software search using the Swiss-Prot database of peptide sequences (amino acid numbering is given in accordance with primary structure of the full length protein)

Start/end	Experimental molecular mass of peptide, Da	Calculated molecular mass of peptide, Da	|Δ|, Da	Number of gaps	Peptide
26-41	1755.02	1755.00	0.015	0	IAIVNVSSIFQQLPAR
47-53	906.42	906.44	–0.022	0	QLENEFK
56-64	1033.47	1033.49	–0.017	0	ATELQGMER
86-94	1090.57	1090.57	–0.001	1	TKLENEVMK
88-94	861.41	861.43	–0.016	0	LENEVMK
88-96	1145.59	1145.59	0.009	1	LENEVMKQR
97-102	711.39	711.34	0.044	0	ETFSTK
103-111	1077.48	1077.48	–0.006	0	AQAFEQDNR
103-112	1233.61	1233.58	0.025	1	AQAFEQDNRR
119-130	1383.75	1383.82	–0.075	2	NKILSRIQDAVK
125-130	672.40	672.38	0.021	0	IQDAVK
136-154	1913.93	1913.90	0.03	0	GGYDVVIDANAVAYADSSK
155-162	873.46	873.48	–0.024	0	DITADVLK

ion peak of IBP-16, the mass spectrum also contained an additional peak at 8.06 kDa, which corresponded to a doubly charged molecular ion.

Automatic solid-phase Edman degradation revealed the N-terminal amino acid sequence of IBP-16 (15 amino acid residues): ADKIAIVNVSSIFQ.

For additional characterization and identification of IBP-16, we determined the isoelectric point (p*I*) of this protein. The isoelectric point was determined by the IEF method in an uncoated capillary [26] with minor modifications of preparation of a mixture of ampholytes and proteins. Since myoglobin has characteristic spectrum at 415 nm, order of appearance of protein fractions was evaluated by the absorbance values at 280 and 415 nm. Using a calibration curve, we calculated the isoelectric point for IBP of 9.2 ± 0.1.

Using data on molecular mass, p*I*, and N-terminal amino acid sequence, as well as the TagIdent program and UniProtKB/Swiss-Prot database, the IBP protein was identified as the Skp chaperone from *Y. pseudotuberculosis*. The amino acid sequence of Skp listed in the database was deduced from the nucleotide sequence of the corresponding gene. During analysis of genomic sequence of *Y. pseudotuberculosis*, no genes encoding any other protein with identical N-terminal amino acid sequences were found.

For validation of the results, we identified the protein by peptide fingerprinting using MALDI-TOF mass spectrometry. We prepared tryptic hydrolysate of IBP-16 and using molecular mass distribution of the tryptic fragments and the Mascot software and the Swiss-Prot database of protein sequences, IBP-16 was also identified as the chaperone Skp from *Y. pseudotuberculosis* (Table 1). Since the Mascot protein identification score is 70, the identification can be considered as correct.

The calculated values of molecular mass and isoelectric point for Skp found in Swiss-Prot (16.106 kDa and 9.33, respectively; Swiss-Prot, P31520 and Q667J8) correspond well with the experimental values determined for IBP-16 in this study (16.14 ± 0.04 kDa and 9.2 ± 0.1).

Binding of Skp chaperone with rabbit and human immunoglobulins. The interaction of Skp with rabbit IgG was investigated using the ELISA method. The IBP was immobilized in a polystyrene plate and the its immunoglobulin binding activity was analyzed using IgG–horseradish peroxidase conjugate.

Skp bound IgG in a concentration dependent manner and saturated behavior of the binding curve suggests specific interaction between Skp and rabbit IgG (Fig. 4a, curve *1*). Similar saturation curves were obtained in the case of *S. aureus* protein A, used as a model immunoglobulin binding protein (Fig. 4a, curve *2*). It should be noted that optimal concentrations of immobilized Skp and protein A required for ELISA determination (determined in pilot experiments) significantly differed; these were 3.5 μM and 4.3 nM for Skp and protein A, respectively. It is known that (other conditions being equal) the optimal protein concentration used for the ELISA method depends on binding constant value. Consequently, we can assume that the K_a value for complex formation between Skp and IgG is lower than that for protein A binding with IgG; the K_a value for the latter reaction varies in the range 10-100 μM^{-1} [33].

For localization of Skp binding sites on an IgG molecule, we used competitive ELISA. These experiments showed that addition of human IgG Fc-fragments inhibited interaction between Skp and human IgG (Fig. 4b).

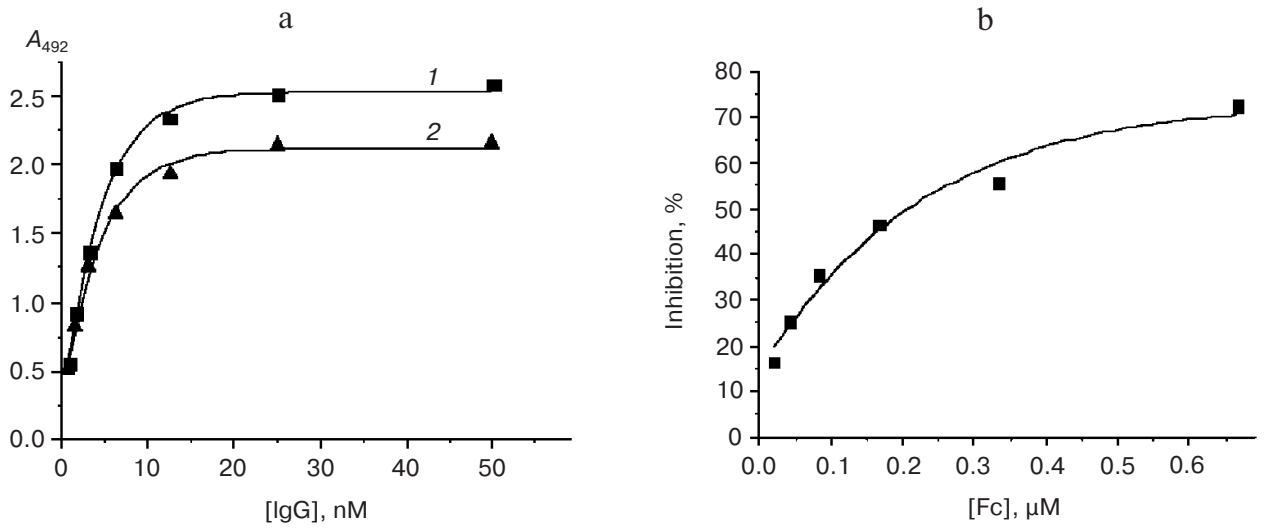

Fig. 4. a) Binding of *Y. pseudotuberculosis* Skp (*1*) and *S. aureus* protein A (*2*) with rabbit IgG conjugated with horseradish peroxidase. b) Inhibition of Skp binding with human IgG by Fc-fragments.

These data suggest that the immunoglobulin Fc-fragment is responsible for binding of *Y. pseudotuberculosis* Skp. It should be noted that maximal inhibition of the binding reaction was just 72%. It is possible that other IgG sites also interact with Skp as demonstrated earlier for IBP from other microorganisms [42]. Using inhibition data, the K_a value of 3.05 μM^{-1} was calculated. According to literature data, the affinity of interaction between bacterial IBP and immunoglobulins varies significantly. For example, *Streptococcus equi* IBP binding with horse IgG was characterized by K_a of 6.96 μM^{-1} [43]. The B fragment of protein A binds rabbit IgG-Fc site with K_a of 3 μM^{-1}, whereas in the case of the native protein A the K_a value was one or two orders of magnitude higher [19].

Computer modeling of *Y. pseudotuberculosis* Skp and its complex with human IgG1-Fc fragment. Results of this study suggest complex formation between *Y. pseudotuberculosis* Skp and IgG1 and involvement of the immunoglobulin Fc-fragment in this binding. For elucidation of possible structure of the complex of Skp and human IgG1, its

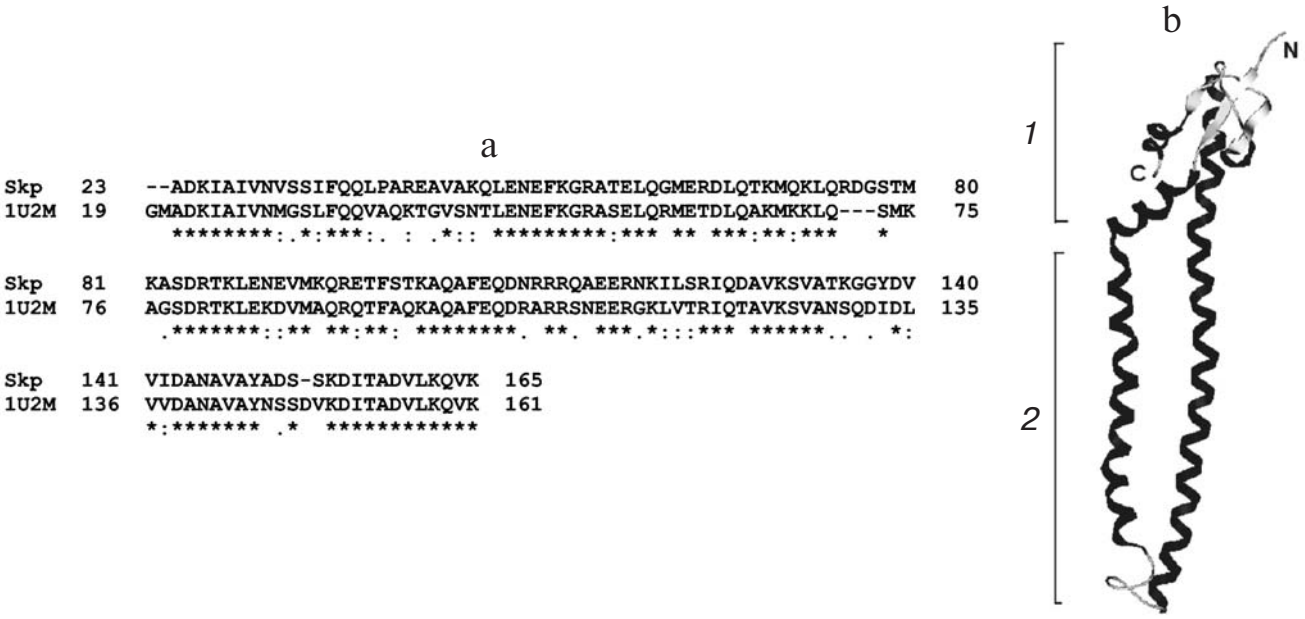

Fig. 5. a) Alignment of amino acid sequences of *Yersinia pseudotuberculosis* Skp protein (serotype O:1b/strain IP31758; UniProt code A7FFH8) and *E. coli* Skp (PDB code 1U2M_C). Indications: (*) identical residues; (:) conservative and (.) semi-conservative substitutions. b) Ribbon diagram of the model of spatial structure of *Y. pseudotuberculosis* Skp.

theoretical model was generated by computer modeling. Since spatial structure of Skp remains unknown, computer modeling studies were started with the prediction of tertiary structure of this protein. Comparative analysis of the primary structure of *Yersinia pseudotuberculosis* Skp (UniProt code A7FFH8) has shown more than 50% identity with amino acid sequences of Skp proteins with known spatial structure. Thus, we chose the crystal structure of *E. coli* Skp [37] (PDB code 1U2M_C), whose amino acid sequence shares 65% identity with *Y. pseudotuberculosis* Skp (Fig. 5a), as a prototype for modeling of spatial structure of the latter protein. A theoretical model of spatial structure of *Y. pseudotuberculosis* Skp was obtained by comparative modeling using the Swiss-Model server (Fig. 5b). Superimposition of all Cα atoms of the model and its prototype showed that root-mean-square deviation is 0.24 Å. The value of potential energy for the *Y. pseudotuberculosis* Skp monomer in vacuum is −10443.9 kJ/mol. Thus, we have generated a highly accurate model of the *Y. pseudotuberculosis* Skp monomer.

The three-dimensional model of *Y. pseudotuberculosis* Skp has folding characteristic to *E. coli* Skp monomer and conservative β-structural sites. Figure 5b shows that the molecule includes two domains: compact preferentially β-structured central domain (1) formed by N- and C-terminal sites and domain (2), which consists of two extended α-helical segments, which form a hairpin with two ends positioned in the central domain. Calculation of molecular surface and electrostatic potential showed that there are negatively and positively charged sites on the surface of the Skp molecule.

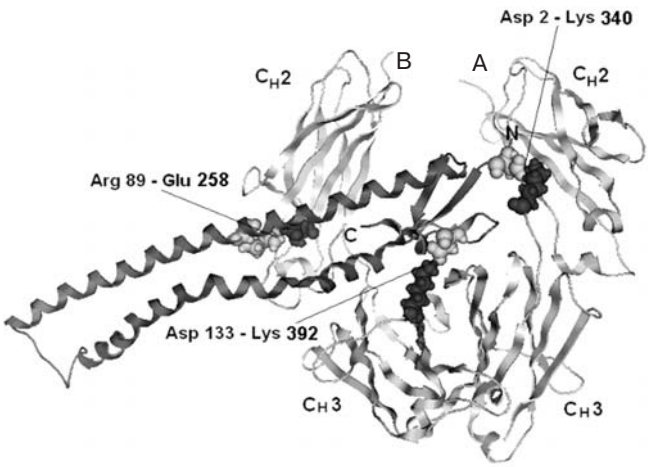

Fig. 6. Theoretical model of the complex of *Y. pseudotuberculosis* Skp with IgG1 Fc-fragment obtained using the GRAMM program. In the ribbon model, Fc-fragment and Skp structures are highlighted with light gray and dark gray and positions of C_H2 and C_H3 domains of Fc-fragment are marked. Amino acid residues forming ionic bonds in the complex are shown as atomic models of light gray and dark light for Skp and Fc-fragment, respectively.

A theoretical model of spatial structure of the complex of *Y. pseudotuberculosis* Skp with human IgG1 heavy chains was obtained by the method of molecular docking using the GRAMM 1.03 program. We found that the most favorable binding site is located at the IgG1 Fc-fragment (Fig. 6). For analysis of contacts, we selected one of 100 calculated complexes; it is characterized by the lowest

Table 2. Interaction of Skp *Y. pseudotuberculosis* with human IgG1 Fc-fragment

Fc-fragment heavy chains	Hydrogen and ionic (*) bonds in the complex	
	Fc CH2–Skp	Fc CH3–Skp
A	GLU333.OE2–ALA1.N	TYR373.OH–LYS132.NZ
	ILE336.N–ASP129.OD2	SER375.OG–ALA128.O
	SER337.OG–ASP2.OD1	ASP376.OD2–TYR127.OH
		LEU398.N–ASP133.OD2
	LYS340.NZ–ASP2.OD1 (*)	SER400.O–LYS140.NZ
	LYS340.O–LYS132.NZ	
B	ARG255.NH2–GLN92.OE1	THR307.OG1–ARG89.NH2
		VAL379.O–GLN14.NE2
	GLU258.OE1–ARG89.NH2 (*)	TYR391.OH–GLN14.OE1
	LYS288.NZ–GLN86.OE1	**LYS392.NZ–ASP133.OD2 (*)**
	ARG301.NH2–GLN104.OE1	

* Residues forming ionic bond are highlighted with a gray background.

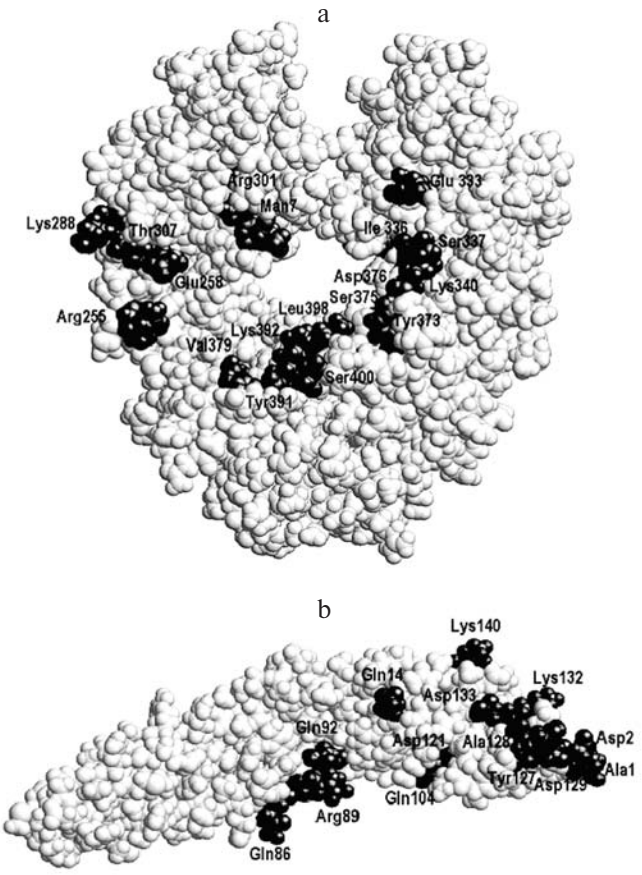

Fig. 7. Amino acid residues of the Fc-fragment forming hydrogen and ionic bonds with *Y. pseudotuberculosis* Skp (a) and Skp residues interacting with Fc-fragment (b). The structures of the Fc-fragment and Skp are shown as atomic models in gray. Residues forming bonds are shown in dark gray.

energy of Skp interaction with Fc-fragment. Energy minimization was performed using the MOE program and the OPLS-AA force field. The value of potential energy of this complex was –42330.17 kJ/mol.

Analysis of contacts showed that the structure of this complex was stabilized by 17 hydrogen bonds and three ionic bonds (Table 2). Skp forms bonds with C_H2 and C_H3 domains of the A and B chains of the Fc-fragment (15 hydrogen and three ionic bonds) and with the carbohydrate site of Fc fragment (two hydrogen bonds). Figure 7 shows residues involved into bond formation in the complex.

Molecular docking of IgG1 heavy chains (A and B) onto *Y. pseudotuberculosis* Skp shows that Fc-domain interaction might involve the C_H1 domain of heavy chains of the Fab-fragments. This might explain incomplete inhibition of binding by the Fc-fragment.

Analysis of contacts between components of the proposed complex revealed apparent charge complementarity on binding surfaces (Asp2, Arg89, Asp133 and Lys340, Glu258, Lys392) (Fig. 6); this suggests the possibility of corresponding molecule orientation during binding based on electrostatic interaction. Amino acid residues involved in complex formation are hydrophilic. Hydrophilicity differs the complex of *Y. pseudotuberculosis* Skp with the Fc-fragment from hydrophobicity of the complex of streptococcal protein A (SpA) with Fc (the contact region of this complex is hydrophobic) [44]. Interestingly, the contact region of the complex SpA–Fv-fragment of IgG is hydrophilic [44].

Comparison of amino acid sequence of *Y. pseudotuberculosis* Skp and amino acid sequences of Skp from other yersinias using the UniProt database showed that this protein is identical to *Yersinia pestis* Skp. *Yersinia pseudotuberculosis* Skp shares 68-94% identity with other Skp proteins of *Yersinia* species. This suggests that Skp of other *Yersinia* species may also exhibit similar immunoglobulin binding properties and that their interaction with IgG1 might also involve the Fc-fragment.

Thus, we have isolated and characterized a periplasmic chaperone Skp/OmpH from *Y. pseudotuberculosis*; its existence was postulated earlier [15, 16]. We have also demonstrated the possibility of non-immune interaction of Skp with rabbit and human IgG (preferentially through the Fc-fragment). Using methods of molecular modeling, we have generated a model of spatial structure of *Y. pseudotuberculosis* Skp and predicted possible structure of its complex with the human IgG1 Fc-fragment. Since results of modeling of this complex reflect probability of its real existence, further experiments are needed to test its correctness.

This work was supported by a grant from the Far Eastern Branch of the Russian Academy of Sciences (No. 06-III-F-05-123).

REFERENCES

1. Thome, B., Hoffschulte, H., Schiltz, E., and Muller, M. (1990) *FEBS Lett.*, **269**, 113-116.
2. Thome, B., and Muller, M. (1991) *Mol. Microbiol.*, **5**, 2815-2821.
3. Chen, R., and Henning, U. (1996) *Mol. Microbiol.*, **19**, 1287-1294.
4. De Cock, H., Schafer, U., Potgeter, M., Demel, R., Muller, M., and Tommassen, J. (1999) *Eur. J. Biochem.*, **259**, 96-103.
5. Schafer, U., Beck, K., and Muller, M. (1999) *J. Biol. Chem.*, **274**, 24567-24574.
6. Qu, J., Mayer, C., Behrens, S., Holst, O., and Kleinschmidt, J. (2007) *J. Mol. Biol.*, **374**, 91-105.
7. Schlapschy, M., Dommel, M., Hadian, K., Fogarasi, M., Korndorfer, I., and Skerra, A. (2004) *Biol. Chem.*, **385**, 137-143.
8. Bulieris, P., Behrens, S., Holst, O., and Kleinschmidt, J. H. (2003) *J. Biol. Chem.*, **278**, 9092-9099.
9. Geyer, R., Galanos, C., Westphal, O., and Golecki, J. (1979) *Eur. J. Biochem.*, **98**, 27-38.

10. Holck, A., and Kleppe, K. (1988) *Gene*, **67**, 117-124.
11. Holck, A., Lossius, I., Aasland, R., and Kleppe, K. (1987) *Biochim. Biophys. Acta*, **914**, 49-54.
12. Holck, A., Lossius, I., Aasland, R., Haarr, L., and Kleppe, K. (1987) *Biochim. Biophys. Acta*, **908**, 188-199.
13. Koski, P., Rhen, M., Kantele, J., and Vaara, M. (1989) *J. Biol. Chem.*, **264**, 18973-18980.
14. Koski, P., Hirvas, L., and Vaara, M. (1990) *Gene*, **88**, 117-120.
15. Chain, P. S. G., Carniel, E., Larimer, F. W., Lamerdin, J., Stoutland, P. O., Regala, W. M., Georgescu, A. M., Vergez, L. M., Land, M. L., Motin, V. L., Brubaker, R. R., Fowler, J., Hinnebusch, J., Marceau, M., Medigue, C., Simonet, M., Chenal-Francisque, V., Souza, B., Dacheux, D., Elliott, J. M., Derbise, A., Hauser, L. J., and Garcia, E. (2004) *Proc. Natl. Acad. Sci. USA*, **101**, 13826-13831.
16. Vuorio, R., Hirvas, L., Raybourne, R. B., Yu, D. T. Y., and Vaara, M. (1991) *Biochim. Biophys. Acta*, **1129**, 124-126.
17. Shrestha, A., Shi, L., Tanase, S., Tsukamoto, M., Nishino, N., Tokita, K., and Yamamoto, T. (2004) *Am. J. Pathol.*, **164**, 763-772.
18. Ezepchuk, Yu. V. (1977) in *Biomolecular Bases of Bacterial Pathogenicity* [in Russian], Nauka, Moscow, pp. 56-63.
19. Widders, P. R. (1991) in *Bacterial Immunoglobulin-Binding Proteins: Microbiology*, *Chemistry*, *and Biology* (Boyle, M. D. P., ed.) Academic Press Inc., San Diego, pp. 375-396.
20. Sidorin, E. V., Kim, N. Yu., Leichenko, E. V., Anastyuk, S. D., Dmitrenok, P. S., Nabereznykh, G. A., and Solov'eva, T. F. (2006) *Biochemistry (Moscow)*, **71**, 1278-1283.
21. Nabereznykh, G. A., Sidorin, E. V., Lapshina, L. A., Reunov, A. V., and Solov'eva, T. F. (2006) *Biochemistry (Moscow)*, **71**, 1284-1288.
22. Ovodov, Yu. S., Gorshkova, R. P., and Tomshich, S. V. (1971) *Imunochemistry*, **8**, 1071-1079.
23. Laemmli, U. K. (1970) *Nature*, **2**, 680-685.
24. Gasparov, V. C., and Degtyar', V. G. (1994) *Biochemistry (Moscow)*, **59**, 563-572.
25. Pinchuk, L. M. (1971) *Zh. Mikrobiol. Epidemiol. Immunobiol.*, **7**, 26.
26. Kilar, F., Vegvari, A., and Mod, A. (1998) *J. Chromatogr.*, **813**, 349-360.
27. Rappsilber, J., Ishihama, Y., and Mann, M. (2003) *Anal. Chem.*, **75**, 663-670.
28. Mikhailov, A. T., and Simirskii, V. N. (1991) in *Immunochemical Analytical Methods in Developmental Biology* [in Russian], Nauka, Moscow, pp. 155-192.
29. Labbe, S., and Grenier, D. (1995) *Infect. Immun.*, **63**, 2785-2789.
30. Catty, D., and Raykundalia, C. (1991) in *Antibodies. Methods* (Catty, D., ed.) [Russian translation], Mir, Moscow, pp. 180-181.
31. Egorov, A. M., Osipov, A. P., Dzantiev, B. B., and Gavrilova, E. M. (1991) in *Theory and Practice of Immunoenzyme Analysis* [in Russian], Vysshaya Shkola, Moscow, pp. 182-183.
32. Bobrovnik, S. A. (2004) *Ukr. Biokhim. Zh.*, **76**, 5-28.
33. Guex, N., and Peitsch, M. C. (1997) *Electrophoresis*, **18**, 2714-2723.
34. Arnold, K., Bordoli, L., Kopp, J., and Schwede, T. (2006) *Bioinformatics*, **22**, 195-201.
35. Schwede, T., Kopp, J., Guex, N., and Peitsch, M. C. (2003) *Nucleic Acids Res.*, **31**, 3381-3385.
36. Kopp, J., and Schwede, T. (2004) *Nucleic Acids Res.*, **32**, D230-D234.
37. Walton, T. A., and Sousa, M. C. (2004) *Mol. Cell*, **15**, 367-374.
38. Berman, H. M., Westbrook, J., Feng, Z., Gilliland, G., Bhat, T. N., Weissig, H., Shindyalov, I. N., and Bourne, P. E. (2000) *Nucleic Acids Res.*, **28**, 235-242.
39. Lindahl, E., Hess, B., and Spoel, D. (2001) *J. Mol. Mod.*, **7**, 306-317.
40. Katchalski-Katzir, E., Shariv, I., Eisenstein, M., Friesem, A. A., Aflalo, C., and Vakser, I. A. (1992) *Proc. Natl. Acad. Sci. USA*, **89**, 2195-2199.
41. Padlan, E. A. (1994) *Mol. Immunol.*, **31**, 169-217.
42. Langone, J. (1982) *Adv. Immunol.*, **32**, 157-241.
43. Lewis, M. J., Meehan, M., Owen, P., and Woof, J. M. (2008) *J. Biol. Chem.*, **283**, 17615-17623.
44. Meininger, D. P., Rance, M., Starovasnik, A., Fairbrother, W. J., and Skelton, N. J. (2000) *Biochemistry*, **39**, 26-36.